JOURNAL OF CATALYSIS 149, 474–485 (1994)

In Situ TEM Investigation of Processes Catalyzed by Pd–Ni Alloy Particles on Carbon Substrates in the Presence and Absence of Oxygen

R. Anton, O. Reetz, and A. A. Schmidt

Institut für Angewandte Physik, Universität Hamburg, Jungiusstrasse 11, D-20355 Hamburg, Germany

Received November 22, 1993; revised May 20, 1994

Processes catalyzed by small Pd–Ni alloy particles (10–20 nm in diameter) vapour-deposited on thin carbon films were investigated by *in situ* experiments in a transmission electron microscope. During exposure to elevated partial pressures of oxygen, and in the regime of high concentrations of Pd, the carbon support was oxidized at the edges of the particles at temperatures from 770 to 870 K, as was apparent by holes developing in the substrate. The activity was highest for pure Pd, and decreased strongly with increasing content of Ni. At concentration values of Ni from 5 to 10 at.%, segregation of Ni and oxidation to NiO was found, while the remaining Pd particle continued to be active in oxidizing the carbon. For further increasing concentrations of Ni, the tendency of NiO segregation decreased, and at about 25%, the particles appeared to be rather stable and no carbon oxidation could be detected any longer. Instead, a weak activity of graphitization of the carbon support was observed, which increased strongly with further increasing concentration of Ni. This was most pronounced for pure Ni, and was apparent in the transmission electron microscopy image by the formation of graphite shells around the particles, and of graphitized areas in the surrounding substrate area by dispersing Ni. At 870 K, this behaviour was found to be similar to the well known case without the presence of oxygen, whereas at somewhat lower temperatures the Ni was oxidized. The dependence on composition of the oxidation or graphitization of the carbon substrate is interpreted as being caused by competitive processes: dissociative adsorption of oxygen on alloys rich in Pd, segregation and oxidation of Ni at the surface of alloys with low concentrations of Ni, and dissolution and diffusion of carbon from the substrate in alloys with medium to high concentrations of Ni, leading to the formation of segregated graphite on the surface of the particles, as well as to graphitization of the substrate.

1. INTRODUCTION

The oxidation of amorphous carbon and graphite by small Pd particles at elevated oxygen partial pressures and temperatures has often been studied as a model system for catalytic processes (see, for example, Refs. (1–4)). Dealing with thin film carbon substrates, transmission electron microscopy (TEM) is well suited for such investigations, as the activity is visualized directly by dramatic morphological and structural changes of the supported metal crystallites, as well as of the substrate. In particular, the oxidation of the carbon film is detected by the formation of holes adjacent to the edges of the metal particles. *In situ* techniques in TEM have been applied by us (5, 6), by Su *et al.* (7), and by Avalos-Borja *et al.* (8) to analyze the kinetics of these processes. Such instrumentation allows continuous observation, while alloy particles are vapour deposited on the substrate, and gas exposure follows. Also, in contrast to *ex situ* techniques, ambiguities due to possible contamination are avoided. At temperatures around 800 K, and in the range of oxygen partial pressures from 10^{-7} to 10^{-5} mbar, the activity of any one particle was found to increase in proportion to its surface area, as well as to the oxygen partial pressure. This behaviour is consistent with the model of dissociatively adsorbed oxygen on the surface of the particles, and diffusion to the metal–carbon interface, where oxidation proceeds. It is conceivable that alloying the Pd with another metallic component with less or no activity would provide valuable insights into the mechanism of oxygen adsorption. In fact, dissociation is expected to depend on the surface composition of the particles, which, however, may be influenced by segregation. Ag, for example, does not absorb oxygen at temperatures above 600 K, nor at a reduced pressure. In our work cited above (6), we found that the addition of only small amounts of Ag to Pd resulted in an even more drastic decrease of activity than expected from the bulk composition. Several effects are discussed in the literature as being responsible for this, such as changes of the electronic structure (ligand effect) due to alloying. Also, a certain number of adjacent Pd atoms could be necessary to allow local dissociative adsorption of an oxygen molecule. Therefore, the more or less statistical distribution of Ag atoms on the surface of the particles is expected to play a major role. In recent work, we have measured the amount of Ag segregation

0021-9517/94 $6.00

on Pd–Ag alloys by surface sensitive analytical methods, namely by Auger electron spectroscopy (AES). Comparison with the activity values resulted in a direct correlation with the surface concentration of Pd (9). This finding, however, neither supports nor excludes the concept of a minimum number of adjacent Pd atoms on the surface.

For the case of Ni at an elevated partial pressure of oxygen, an oxidation reaction with carbon or graphite substrates has not been reported to occur at temperatures up to 800 K. However, catalytic gasification of graphite by nickel was observed at temperatures above 1050 K, and at high hydrogen partial pressures (10). A hydrogenation reaction apparently results in formation of methane. On the other hand, transition metals are known to accelerate the graphitization of carbon (11, 12). This was observed for Ni particles on amorphous carbon to start at temperatures as low as about 700 K (13). These authors state that graphitization proceeds in a vacuum, as well as under a hydrogen atmosphere. It is assumed that the mechanism consists of the breaking up of carbon–carbon bonds, dissolution of carbon atoms in the metal, bulk diffusion, and segregation as graphite layers at the surface.

For alloys, as was mentioned above, the catalytic activity and selectivity may be strongly influenced by segregation effects at elevated temperatures. These, in turn, may depend not only on the difference in surface energy of the components, but also on the environment. For example, for the system Cu–Ni, segregation of Cu is expected to occur in a vacuum due to the lower surface energy of Cu than of Ni. At elevated partial pressures of oxygen, however, strong segregation of Ni and formation of NiO at the surface has been found (14). Similarly, for Pd–Ni, segregation of Ni and formation of NiO have also been reported (15).

The aim of the present study was to investigate the dependence on composition of the activity for carbon oxidation or graphitization, respectively, by supported Pd–Ni particles. In particular, the influence of the formation of NiO on the reaction with carbon was of interest. A further question is that of whether the rate of carbon oxidation correlates with the surface concentration of Pd in a similar manner as was found for Pd–Ag in our earlier work. This is currently investigated by surface analytical methods, and will be discussed in another paper (16).

2. EXPERIMENTAL

The experiments were performed in a modified, conventional transmission electron microscope (TEM, Philips EM 400), which was equipped with an additional ultrahigh vacuum chamber attached to the specimen goniometer stage of the microscope. Details have been described in earlier papers (6, 17). The chamber was differentially pumped by a turbomolecular pump, in series with a diffusion and a forepump. It contained two Knudsen-like evaporation sources for Ni and Pd, shutters, a quadrupole mass filter, an ionization gauge, and a gas inlet system. While a base pressure in the chamber in the mid 10^{-9} mbar range was reached, a value of about 10^{-8} mbar was estimated for the specimen surrounding, where a cold trap was cooled with liquid nitrogen. Recently, the conventional turbopump at the chamber has been replaced by a type with magnetic bearings, providing an extremely low level of vibrations without frequent maintenance (18).

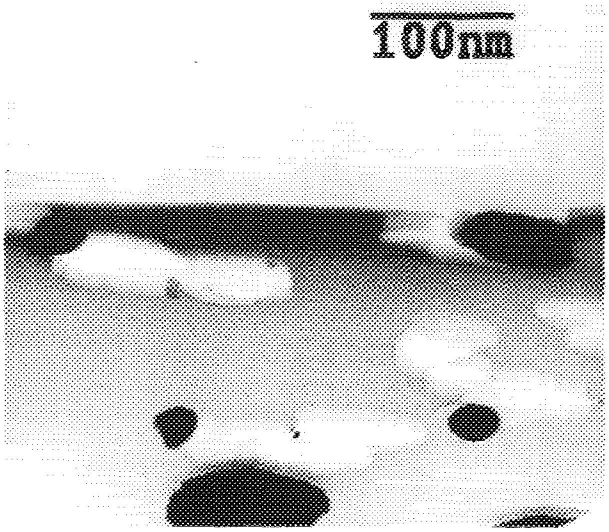

FIG. 1. Perspective view at a small angle onto a carbon film, which was broken and bent over. The cross section can be best seen in holes which had been produced by catalytic oxidation of the carbon by Pd particles. The walls at the edges of the holes are mostly more or less vertically oriented with respect to the film, while thinned areas are wedge shaped.

Microscope images were usually collected via an intensifier CCTV chain by a video tape recorder. Thus, the electron illumination dose was substantially reduced. Moreover, as we were normally working at medium magnifications up to 100,000×, the beam density needed to record images at TV rate was only about 0.1 A/cm^2. In fact, we have not found any indications for irradiation artefacts by comparing illuminated with nonilluminated areas on the specimen. Micrographs were also intermittently recorded on film, at somewhat increased beam densities. Digital image enhancement and quantification was performed with an image analyzing computer.

Thin film substrates of amorphous carbon of 10- to 20-nm thickness were prepared *ex situ* in the following way. Carbon was vapour deposited on mica from an electron beam gun in a high vacuum system. The thickness was controlled by a quartz crystal microbalance and by optical

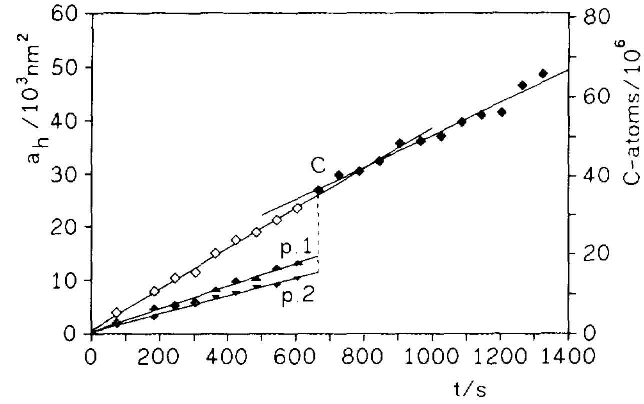

FIG. 2. Increase of the hole areas around two Pd particles, p.1 and p. 2 (solid triangles), and of the sum of both hole areas (open rhombs). When compared to this, note the slower increase of the hole size after coalescence (marked by "C," solid rhombs). Solid lines are least-square fits.

interference measurements, and was reproducible to within less than 10%. The density of these films is close to that of graphite (2.25 g/cm^3). The thickness could occasionally also be measured in the TEM on a broken film, exposing a cross-section at the edge of a hole (see Fig. 1). After floating off in water, the films were picked up on gold TEM grids. A grid was mounted in the heatable specimen holder. After inserting into the microscope, the sample was outgassed at 900 K for several hours in order to remove most of the water embedded in the film. Alloy particles were grown at substrate temperatures around 670 K by simultaneous deposition of Pd and Ni at constant rates, which were monitored by the mass filter. Thus, the composition in the deposit was reproducible to within 2 at%. It was concluded from earlier experiments (see, for example, Refs. (19–21)) that particles with uniform composition (apart from possible segregation effects) were obtained in this way. In particular, the sharpness of the rings in the electron diffraction patterns suggested virtually homogeneous compositions, as the lattice parameters of Pd and Ni differ by more than 10%, and the metals form continuous solid solutions with monotonic dependence of the lattice parameter on composition. Significant variations within any one specimen would be apparent by smearing out of the rings. The compositions of the samples were independently measured by X-ray analysis (EDX). For calibration, test specimens were produced with known amounts of the components, which had been determined by quartz crystal and optical interference measurements. The absolute error limits in composition were about ±2 at.%, but differences between specimens of less than 3 at.% were easily detectable. During metal deposition, the residual gas pressure was in the mid 10^{-8} mbar range. At condensation rates in the range from 10^{12} to 10^{13} atoms/(cm^2 s), isolated particles with sizes up to about 20 nm were obtained within 30 to 40 min, when the deposition was stopped. Up to this point, virtually no interactions of the alloy particles with the substrate were observed. The results of the subsequent gas exposure experiments will be described in the following section.

3. RESULTS

3.1. *Palladium*

The observations on pure Pd particles were similar to those reported in our earlier paper (6), and are briefly summarized here for comparison only. After increasing the temperature up to about 860 K, oxygen was admitted to a total pressure of 5 × 10^{-6} mbar, at which pressure most of the particles started to become mobile and frequently changed their shapes, while erosion of the carbon film was apparent at the particle-to-substrate interfaces. During this process, the particles exhibited a fluctuational behaviour but continuously exhibited Bragg contrast, and thus remained crystalline. The micrograph in Fig. 1 shows a perspective view, where the carbon film was bent over so as to reveal the morphology of the holes in the carbon film in more detail. Especially noteworthy are the wedge-shaped edges in some places, which appear as thinned areas in normal projection. The rate of carbon oxidation was evaluated from measurements of the increase in size of the holes. With known thickness of the carbon films,

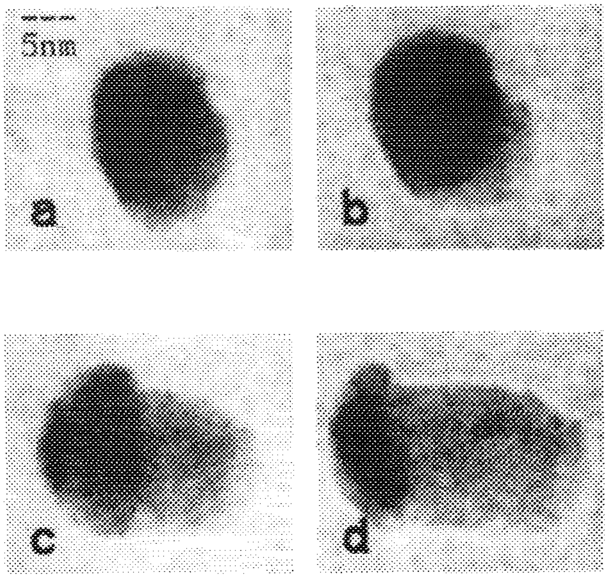

FIG. 3. Video sequence of the oxidation of a Ni particle on carbon. T = 620 K, $p(O_2)$ = 5 × 10^{-6} mbar. Precipitation and spreading of NiO on the support is apparent at the right hand side of the particle. In (a), the original Ni particle is shown, while images (b), (c), and (d) were taken at 3, 6, and 12 min after admission of oxygen.

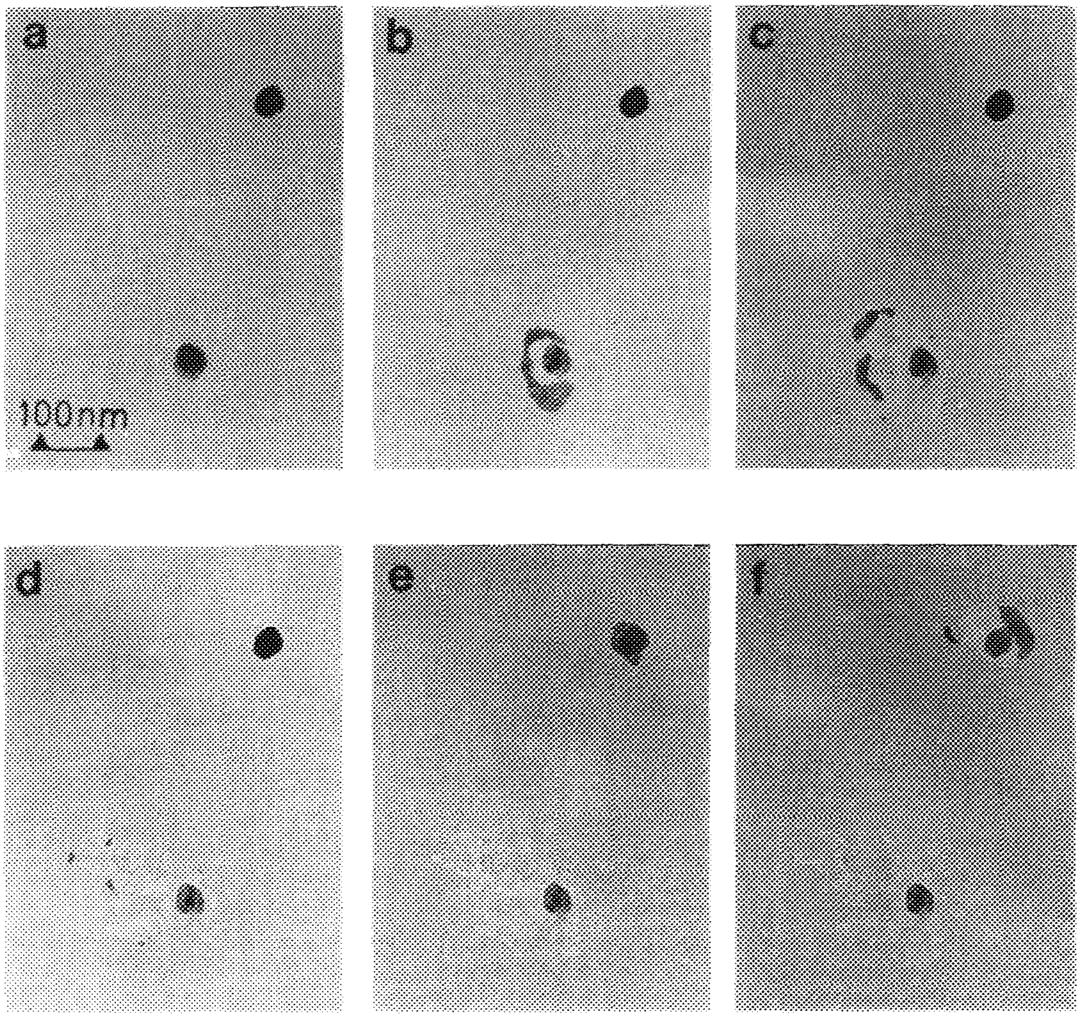

FIG. 4. Sequence of micrographs, showing the reaction of Ni particles with the carbon support film. $T = 870$ K, $p(O_2) = 5 \times 10^{-6}$ mbar. t = (a) 1, (b) 2, (c) 5, (d) 10, (e) 24, and (f) 29 min after admission of oxygen. Note the spreading and dispersion of metal in the surroundings, as well as the reduction in size of the original Ni particles with concomitantly grown graphite shells.

ranging from 10 to 20 nm, the activity was calculated as the number of carbon atoms being removed per unit of time. The contribution of the thinned areas was estimated by assuming that half of the thickness of the original carbon film was affected. In all respects, the results corresponded to those reported in earlier work (6). In particular, the activity was measured to be roughly constant for any one particle and was proportional to its surface area. Additional support of this finding was obtained from coalescence events of neighbouring particles. In Fig. 2, the growth of holes in the carbon film is plotted vs time for two initial particles, as well as for the sum of both and for the particle resulting after coalescence. The increase of the sum of the hole areas produced by the initial particles is steeper than the corresponding increase of the hole area produced by the larger particle after coalescence. This is expected for the case where the activity is determined by the surface area of the catalyst and where the shape of the particles virtually does not change with coalescence. In fact, roughly spherical shapes are observed for the two particles before coalescence and for the single particles afterwards. The ratio of the slopes of the lines for the sum of the initial particles and for the coalesced particle was calculated to correspond to the respective ratio of the surface areas within 5%.

3.2. Nickel

Under similar conditions as for Pd, particles of pure Ni behaved quite differently, especially with regard to the dependence on temperature during admission of oxygen. In contrast to Pd, which did not show any reaction with

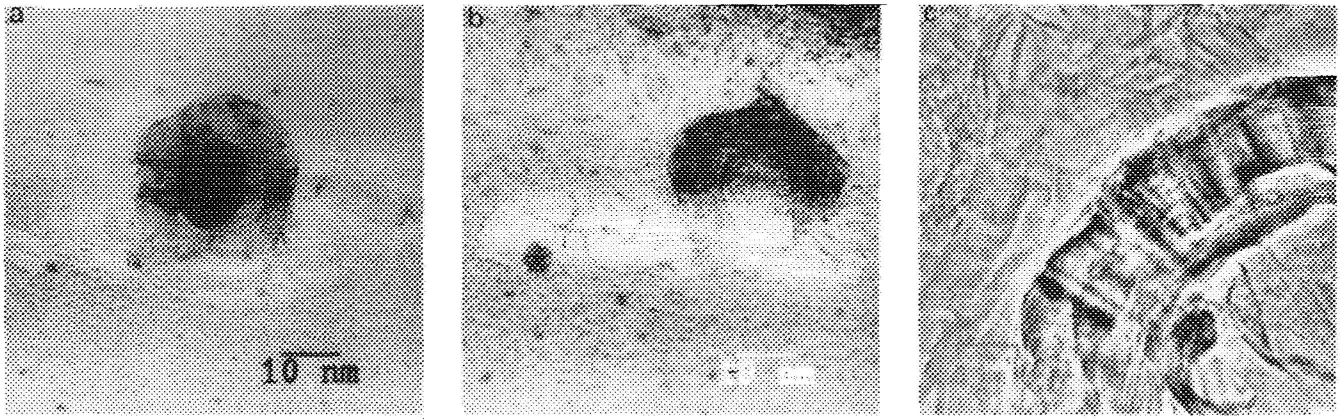

FIG. 5. (a) Micrograph of a Ni particle enclosed in a graphite shell on a carbon film substrate. The reaction temperature was 800 K. The viewing angle is about 30 degrees off the carbon film plane. The somewhat lighter appearance of the area around the graphite bulb indicates thinning or graphitization of the carbon film. Small dark patches are finely dispersed Ni particles. (b) Similar to (a), after the Ni had been ejected out of the graphite shell. During dispersion on the carbon, graphitized trails had been produced. (c) Lattice image of a graphite shell at higher magnification.

oxygen in our experiments, Ni was oxidized to NiO when oxygen was admitted to a total pressure of only 5×10^{-6} mbar, while the temperature of the sample was at around 600–700 K, as is illustrated in Fig. 3. At 770 K, spreading and disintegration of the oxide proceeded at high speed. When the temperature was further increased to 870 K, before the Ni was completely oxidized, remaining metal particles started to graphitize the substrate, which became apparent by characteristic contrast features and by diffraction.

On the other hand, when oxygen was only admitted *after* the temperature of the sample was increased to 800 K, no oxidation of the Ni was observed. Instead, the particles started to graphitize the amorphous carbon, and this did not depend on the presence of oxygen. The behaviour was quite similar to that described already by Lamber *et al.* (13), although those experiments were not done *in situ* in the TEM. Several stages of the interaction could be distinguished, as is shown in the series of micrographs in Fig. 4. Initially, the reaction became visible, as shells with light contrast developed on the surfaces of the particles. These were already present on both particles in Fig. 4a, but are not apparent in the print because of the limited resolution in contrast. Interestingly, the *in situ* observations proved that this shell grows inwards, as can be seen in the following images, while its outer circumference preserves the initial shape of the original particle and the metal core shrinks.

High resolution TEM images and diffraction analysis revealed that the shell consists of layers with spacing of about 0.335 ± 0.005 nm, which corresponds to the literature value of 0.336 nm for the interplanar spacing of the (002) lattice planes of graphite (see Fig. 5c). Obviously, the graphite lattice is preferentially oriented with the *c*-axis perpendicular to the particle surface. This may be the result of epitaxial growth on crystallographic facets of the metal particles. By growing into the particle, the Ni is more or less rapidly driven out at the base of its self-produced encapsulation. It was often observed that, at a certain instant, the Ni core was suddenly ejected out of the shell and dispersed on the surrounding carbon film, which was then graphitized, also. This is illustrated in Figs. 5a and 5b.

Generally, the Ni diffused out in a more gradual manner, such that a thin layer of metal with relatively light contrast expanded from the particle edges on the sur-

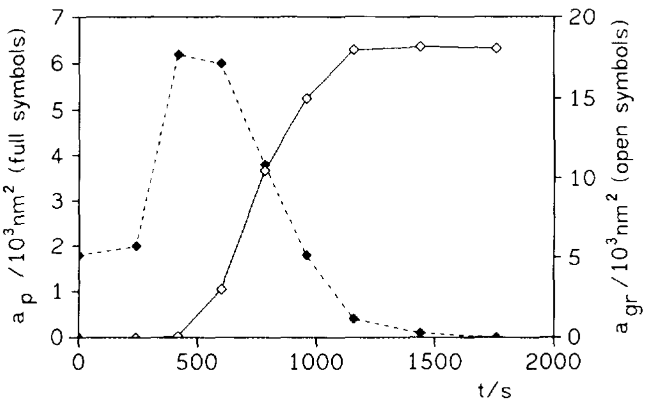

FIG. 6. Increase with time of the graphitized area a_{gr} in the carbon support film, produced by a Ni particle, or its fragments (open symbols, right hand ordinate), and development of the projected area a_p of the metal (full symbols, left hand ordinate). For further explanations, see text.

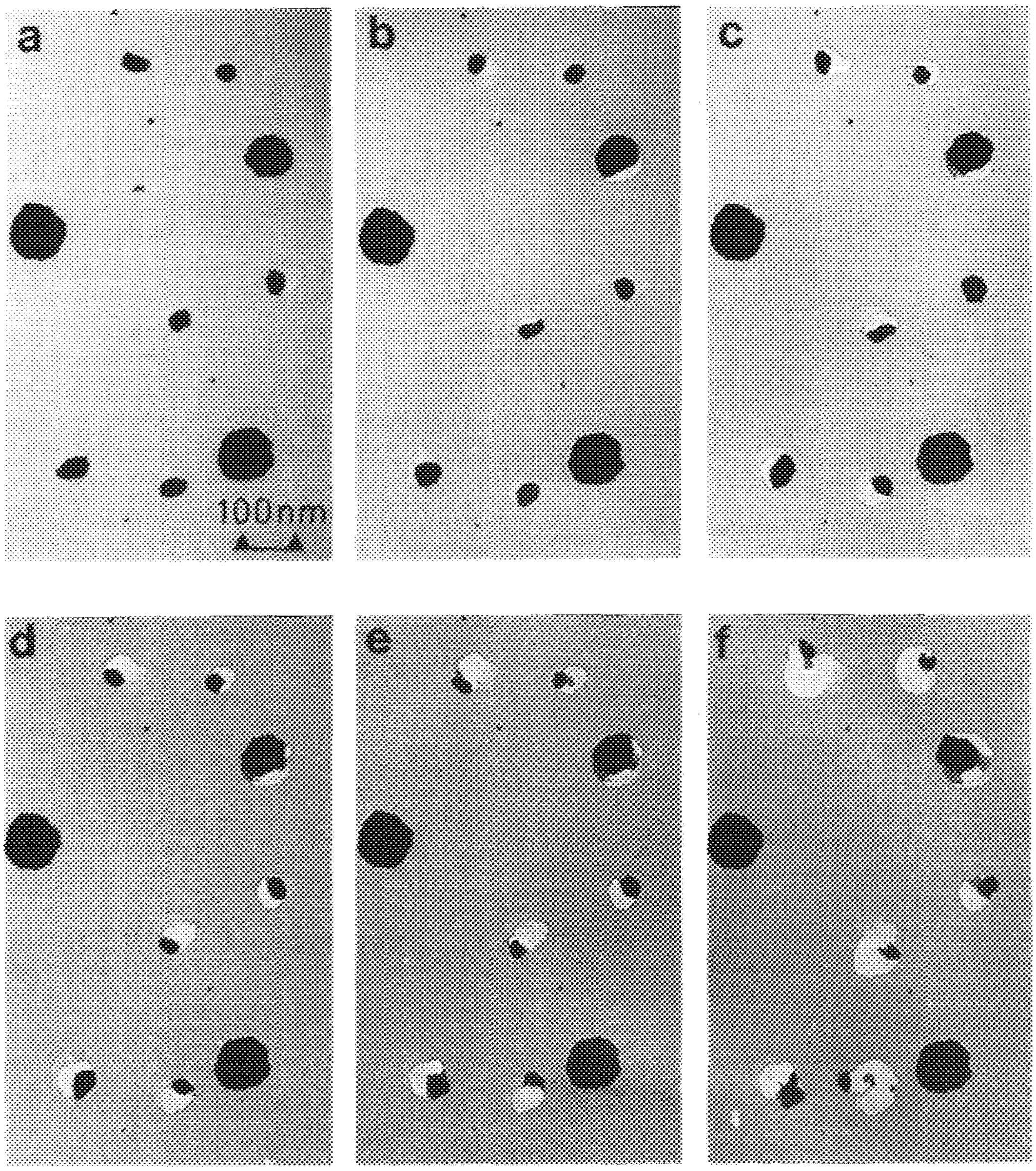

FIG. 7. Sequence of electron microgrphs, taken during catalytic action of alloy particles with composition Pd93–Ni07 (numbers in at.%). t = (a) 1, (b) 5, (c) 9, (d) 13, (e) 17, and (f) 33 min after admission of oxygen. T = 860 K, $p(O_2) = 5 \times 10^{-6}$ mbar. Note the formation of precipitates at most of the particles.

rounding carbon support. While spreading further, this patch of metal film eventually separated from the site of the original particle and, moving away, trails with lighter contrast became apparent on previously covered areas. In later stages, the metal film disintegrated into smaller particles, with correspondingly reduced activity, which finally ceased when the metal was totally dispersed on or in the carbon. High resolution imaging and diffraction revealed that the trails consisted of graphitized carbon. Shading or edges in these areas as well as abrupt contrast changes were caused by discontinuous movements of the particles, with frequent stops and changes of the direction of propagation, as was observed *in situ* during the reaction. Apparently, during any one stop, more or less vertical graphite layers were built up at the edges of the particles. These caused a somewhat increased contrast an were suitable for lattice imaging.

In Fig. 6, as a representative example, the increase of the graphitized area, produced by an individual particle, as well as its projected area, are plotted vs reaction time. Apparently the reaction started with some delay after the temperature was abruptly increased from 670 K (this was

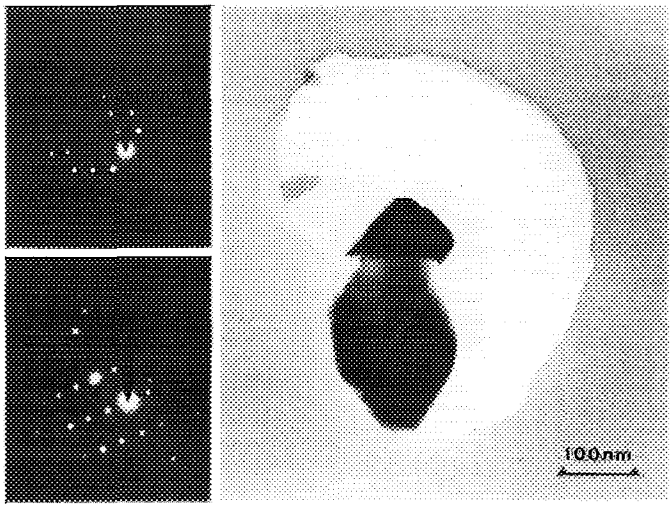

FIG. 8. Micrograph of a particle with nominal composition Pd93–Ni07, taken at higher magnification, showing precipitation. The microdiffraction patterns stem from the individual grains. The upper one consists of NiO, the lower one of virtually pure Pd.

the temperature of deposition of the particles, at which no noticeable reaction occurred within prolonged time) to 870 K. This is caused by the initial formation of a graphite encapsulation, as was mentioned above. While the Ni subsequently diffuses out from its shell and spreads on the substrate, the graphitization speed increases, but is reduced in late stages, as dispersion of the Ni takes place. Disintegration of the Ni particle was taken into account by summing up the projected areas of the fragments, as well as by taking the sum of the respective areas, which had been graphitized by them. It is not clear yet what happens to the Ni. Possibly, it is totally dispersed on an atomic scale in the graphitized areas. On the other hand, we did not find any contrast features which would support this idea. Also, diffraction analysis did not show indications for the formation of Ni carbide.

3.3. Pd–Ni Alloy Particles

In the range of Ni concentrations of up to about 15 at.%, catalytic oxidation of the carbon support film was observed, but the activity decreased sharply, as the Ni content increased. In addition, in the range of low contents of Ni, precipitation of NiO particles was frequently observed. This can be seen, for example, in the series of micrographs in Fig. 7, obtained during the reaction cycle of alloy particles containing about 7 at.% of Ni. Two effects are remarkable. First, comparing the time scale with that for pure Pd, the oxidation of the carbon initially proceeds significantly more slowly at otherwise similar experimental parameters. Second, precipitates which were identified as NiO (see below) grow at the edges of the particles. This is most clearly seen at later times. Often, the precipitates are separated from the original particles, as can be seen in Fig. 7f). The NiO particles did not catalyze the oxidation of the carbon, while the main parts of the original particles even seem to increase their activity. This is reasonable, as their composition approaches pure Pd by segregation of Ni. This is supported by electron diffraction data.

Figure 8 shows the result of precipitation in more detail. The larger portion of the particle probably consists of mostly, when not pure, Pd, as was suggested by the high activity of carbon oxidation. In fact, microdiffraction data obtained from the two grains in the particle yielded a difference of the lattice constants of about 7.5 ± 0.1%, which is very close to the literature value of 7.46%, with lattice parameters of $a_0 = 0.389$ nm for Pd and $a_0 = 0.418$ nm for NiO. The same result was obtained from selected area diffraction analysis of large areas of the specimen containing many particles, such as to produce superimposed ring patterns of the two components. Also, calibration in absolute terms resulted in fairly good agreement.

The tendency of NiO precipitation was found to decrease with further increasing Ni content. At a concentration of 10 at.%, NiO particles were found less frequently. Instead, most of the alloy particles exhibited pronounced changes of their shapes during the reaction, as is illustrated by the sequence of micrographs in Fig. 9. The parameters were about similar to those given before. Here, the reaction of the alloy proceeded even more slowly than was found for that with 7% Ni. Also, in contrast to the above cases, the carbon film was often only thinned and the area of the holes being formed was smaller, although the carbon film thickness was the same. Most conspicuous is the increased wetting of the substrate by the alloy particles, which is apparent by the spreading of the metal along the edges of the holes in the carbon film. The reduced contrast when compared to that of bulk particles suggests that their shapes had transformed into flat films with reduced thickness. In Fig. 10, the increase of the converted substrate area, e.g., the amount of oxidized carbon, is plotted vs time. The data points represent average values from numerous particles, being normalized to their projected ares. For comparison, the data for pure Pd are also plotted. It is evident that the activity of the alloy is reduced. As segregation of NiO was not significant here, this reduction is in fact attributed to the Ni content in the alloy particles.

Similar investigations had also been performed with compositions of Pd85–Ni15, Pd75–Ni25, and Pd50–Ni50. In Fig. 11, the varying behaviour of the alloy particles from pure Pd to pure Ni is compared. In all cases, the experimental parameters were about the same. From series of micrographs, obtained during any one reaction cycle, representative images were collected which had

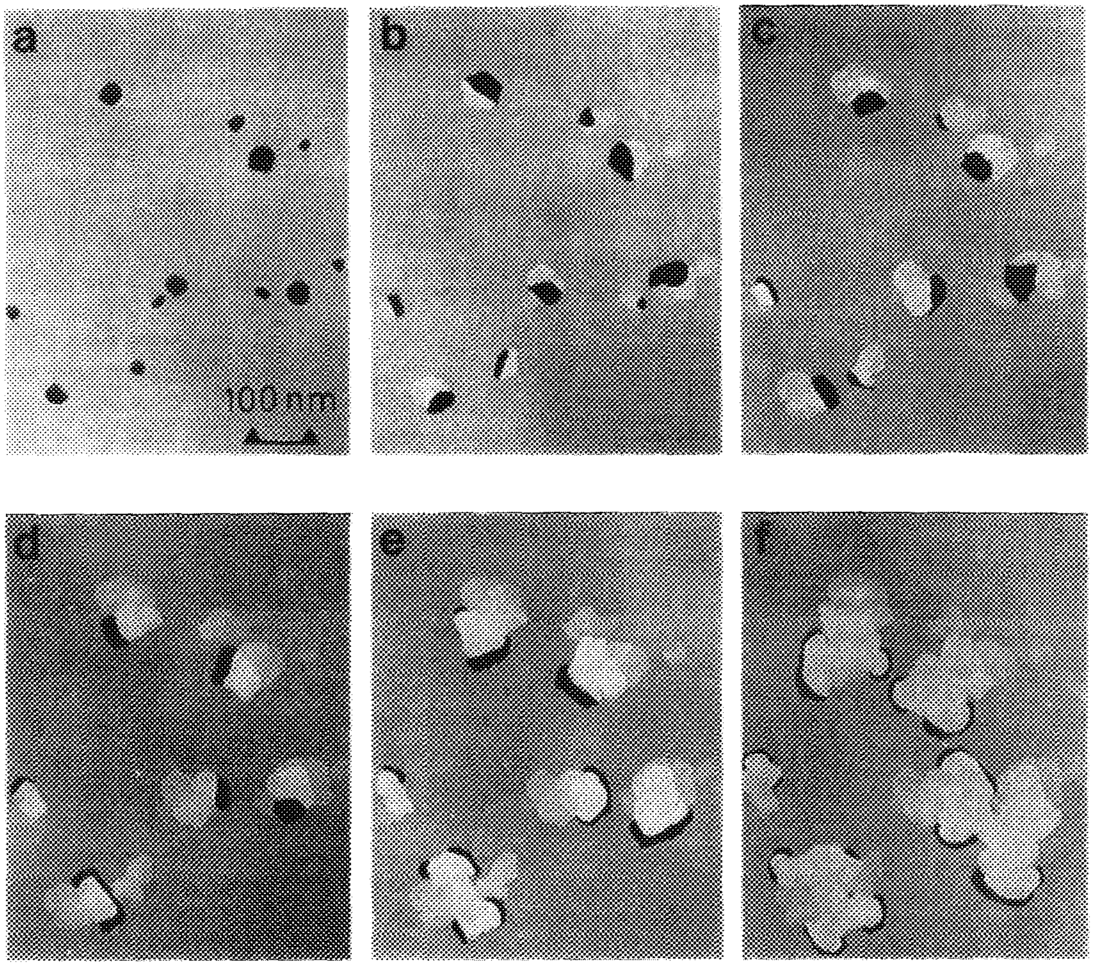

FIG. 9. Catalytic action of alloy particles with composition Pd90–Ni10 (at.%). t = (a) 1, (b) 5, (c) 9, (d) 13, (e) 18, (f) 33 min after admission of oxygen. T = 870 K, $p(O_2) = 5 \times 10^{-6}$ mbar. Note the strong wetting of the carbon support by the alloy particles.

been taken at similar times after the start of the reaction. In the regime of high concentrations of Pd, the decreasing carbon oxidation activity with increasing content of Ni is well illustrated, as is, in the regime of higher concentrations of Ni, the decreasing graphitization activity with increasing content of Pd. A minimum of any activity occurs around a concentration of 25 at.% Ni. These particles were stable and virtually did not exhibit changes in shape or contrast, as was typical for active particles with other compositions. Whereas no oxidation activity at all was observed, only a very weak activity of graphitization of the support was found, which only became apparent after much longer times than usual.

In Fig. 12, the activities of oxidation and graphitization are quantitatively compared. Here, relative activities are plotted vs the composition of the particles. The data were obtained from the converted substrate areas per unit of time and were normalized to those of the respective pure elements, which means Pd for oxidation and Ni for graphitization. It should be noted that these results refer to a temperature of about 870 K. It was concluded from additional, nonsystematic experiments at below and above this value that the composition of minimum activity may depend on temperature.

4. DISCUSSION

The mechanism of catalytic oxidation of carbon by supported Pd particles is explained by dissociative adsorption of oxygen molecules on the metal surface, diffusion, and reaction with the carbon at the interface. The proportional increase of activity with particle surface area indicates that surface and not bulk processes of oxygen are rate limiting under our experimental conditions. This was especially supported by the change of activity of coalescing particles, in proportion to the respective surface areas.

A decrease of activity is reasonable for alloy particles with increasing content of an inactive component. In fact,

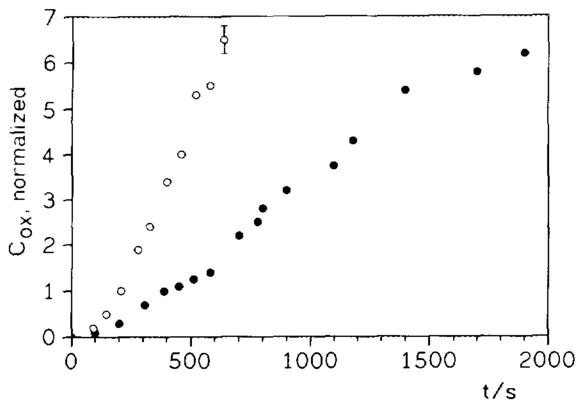

FIG. 10. Increase with time of the amount of oxidized carbon, C_{ox}, around alloy particles with composition Pd90–Ni10 (at.%) (full circles). For comparison, data for pure Pd are also plotted (open circles). In all cases, the experimental conditions were the same as given in Fig. 9. Each data point represents an average from values for several particles, being normalized to their respective surface areas, assuming spherical shapes.

in our earlier work on Pd–Ag alloy particles (6), we observed an even stronger decrease of activity than was expected from the bulk composition. This was caused by surface segregation of Ag, which we have independently investigated with surface analytical methods (9). The driving force is the lower surface energy of Ag than of Pd. This effect resulted in a direct correlation of activity with the surface concentration of Pd on the particles within the error limits. However, the case of Pd–Ni alloys is different, in that the surface energy of Ni (2.08 J/m^2) is higher than that of Pd (1.743 J/m^2, the values for both metals being given for their respective melting points (22)), such that the latter would be expected to segregate. In fact, this is what we have found by Auger electron spectroscopy investigations under UHV conditions (16). In contrast, at a partial pressure of oxygen of around 10^{-6} mbar, segregation of Ni was evident, and the Auger electron spectrum exhibited a rather high peak of oxygen also, which was presumably due to the formation of NiO. The reason for this behaviour is assumed to be the stronger affinity of oxygen to Ni than to Pd. Absorption of oxygen would then lead to oxidation of the Ni, as the enthalpy of formation of NiO (−57.3 kcal/mole at 298 K) is much lower than of PdO (−20.4 kcal/mole) (23). Interestingly, precipitation of NiO occurred most effectively at low concentrations of Ni, but this tendency decreased for further increasing content of Ni, and at around 25 at.%, no formation of oxide was found any more. These findings correspond to electron spectroscopy and diffraction studies of other authors, which resulted in the formation of an NiO overlayer on Pd–Ni alloy foils after heat treatment at 870 K and under an oxygen partial pressure of 3×10^{-5} mbar (15). Also, an increase of the Ni oxidation rate with increasing content of Pd was reported. This enhancement can be explained by the catalytic dissociation of oxygen in the presence of Pd at the alloy surface.

Formation of NiO apparently implies the following effects. As the oxide does not contribute to catalytic oxidation of carbon, at least under our exprimental conditions, the activity of the alloy particles is reduced corresponding to the actual surface concentration of Pd. On the other hand, at least for bulk concentrations of Ni in the range around 5–15 at.%, Ni diffuses out from the particles and reacts with oxygen, such that oxide precipitates are formed, while the remaining fraction is left as virtually pure Pd. This means that its activity increases again, as we have actually observed. This interpretation is also supported by results of the above-cited authors, namely that an alloy with bulk concentration of Ni of 12 at.% still showed some Pd at the surface after prolonged oxygen exposure. They argue (15) that the NiO might be porous, with some Pd being embedded. Indeed, our TEM results suggest that the alloy surface is not continuously covered with NiO, but that oxide precipitates locally, leading to surfaces of virtually pure Pd elsewhere.

With further increasing concentration of Ni in the particles, the decreasing activity in carbon oxidation as well as in precipitation of NiO is apparently caused by the increasing diffusive interaction with carbon. For pure Ni, the mechanism of graphitization of amorphous carbon is explained by diffusion of carbon atoms in the bulk and segregation of graphite layers at the surface. In a first approximation, this process does not depend on the presence of oxygen in the environment, as was realized in our experiments. For the case of alloys with Pd, it seems that the diffusion coefficient is reduced by an increasing concentration of Pd. At least we did not find any indications for dissolution of carbon in pure Pd under our experimental conditions. However, this conclusion would not correspond to measurements of the diffusivity of C in Pd and Ni by Yang *et al.*, who reported values of $6.5 \times 10^{-8}/cm^2s$ and $4 \times 10^{-9}/cm^2s$, at 975 K, respectively (24). On the other hand, it is doubtful whether these results are applicable for our case of isolated crystallites, as they have been obtained for polycrystalline materials, for which diffusion along grain boundaries is known to play a major role. Also, the temperature was considerably lower in our experiments. If for bulk crystals the diffusivity of C were higher in Pd than in Ni, one would expect an even stronger effect of carbon or graphite segregation at the surface, which we did not observe.

In alloys, a slight carbon diffusion may already take place at rather low concentrations of Ni. This may have two competing effects in the presence of oxygen. At first, carbon segregating at the surface blocks the formation of Ni oxide. On the other hand, as diffusion of carbon atoms in the bulk alloy is slow, segregating carbon will more or

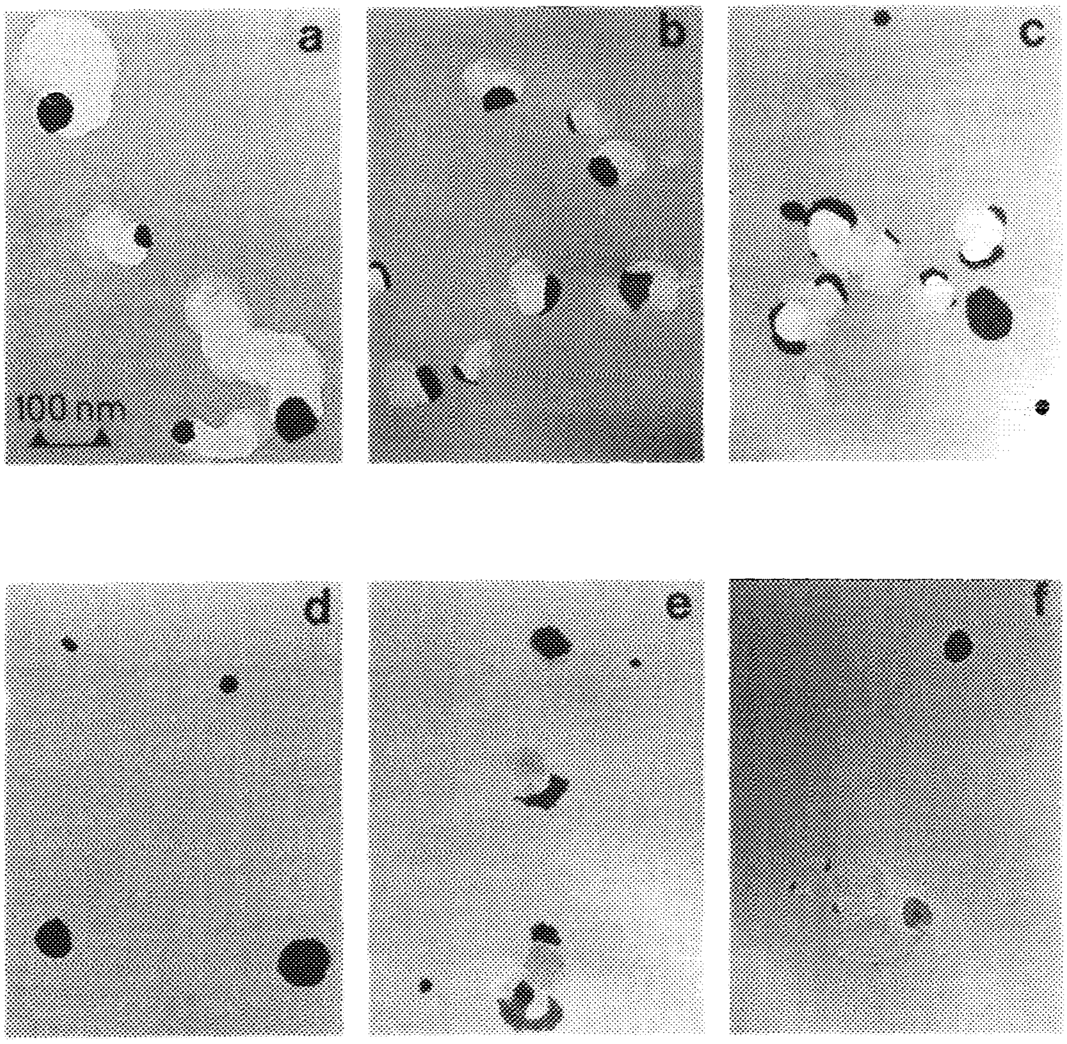

FIG. 11. Micrographs of alloy particles of different composition, each taken at about 9 min from sequences similar to those shown in Figs. 1, 5, 9, and 11. The temperatures were between 860 and 870 K, and the oxygen partial pressure was 5×10^{-6} mbar. The compositions are: (a) Pd100, (b) Pd90/Ni10, (c) Pd85–Ni15, (d) Pd75–Ni25, (e) Pd50–Ni50, and (f) Ni100. All numbers represent at.%. Note especially the virtually inactive particles in d.

less rapidly be oxidized and removed from the surface. Thus, virtually no continuous graphite layers may be formed. This is especially reasonable, as oxygen molecules are still dissociatively adsorbed due to the remaining content of Pd. It appears that the minimum of activity at a bulk concentration of Ni of about 25 at.% in the particles is the result of a sort of equilibrium between tendencies for segregation and oxidation of carbon on the one hand, and oxidation of Ni and blocking by carbon on the other. The composition where this minimum occurs may depend on temperature. The sticking coefficient of oxygen molecules decreases with increasing temperature, while the diffusion coefficient of carbon in the bulk increases. Therefore, a shift to lower concentrations of Ni is expected for the composition with minimum activity, when the temperature rises.

For higher concentrations of Ni, carbon diffusion dominates, such that oxidation of surface Ni is completely blocked by segregation of graphite layers. This would also explain the contrasting findings by other authors (see Ref. (15), who reported on the formation of NiO from bulk foils of pure Ni, as well as of a range of Pd–Ni alloys, at 870 K, although at a somewhat higher oxygen partial pressure of 5×10^{-5} mbar. In our case, oxidation of the Ni is suppressed by the presence of carbon. Only at somewhat lower temperaturs, did formation of NiO occur due to slower diffusion of carbon in the metal. At temperatures around 770 K, at a partial pressure of oxygen of

5×10^{-6} mbar, the oxide seemed to be partly reduced or dissolved in the remaining Ni, as the typical contrast features of segregated phases disappeared. Also, some oxide may be dispersed in or on the substrate film on an atomic scale. Such dispersion of supported metal oxide particles during annealing under oxygen is a phenomenon which is often found for supported catalyst particles under various conditions (25). In any case, it seems that dissociative adsorption of oxygen, being necessary, and taking place on Pd and on alloys with rather high concentrations of Pd, is not or at least much less effective on Ni or on alloys rich in Ni, under our normal experimental conditions.

Regarding the disappearance of Ni during catalytic graphitization of the carbon support, which did not depend on the presence of oxygen, at 870 K, we can only speculate about several possibilities. Dissolution in finely dispersed form, or even formation of carbide, was not definitely supported by TEM and diffraction analysis, although redispersion of supported metal catalysts upon heating in various atmospheres is a commonly known phenomenon (25). Formation of Ni carbonyl, $(Ni(CO)_4$, which would evaporate under our conditions, appears to be unlikely, as this would usually require a higher partial pressure of CO, which was in our case below 10^{-7} mbar (26). Alternatively, evaporation of the metal may be possible, as a decrease of the melting point and an increase of the vapour pressure is common for small particles. In addition, the actual temperature of an individual particle could be increased by the energy being released by its catalytic action. This could further increase the vapour pressure.

5. CONCLUSION

Our *in situ* TEM investigations of the kinetics of catalytic processes of Pd–Ni alloy particles on carbon support films have yielded valuable insights into the mechanisms of the interactions with carbon, and oxygen. At a partial pressure of oxygen of 5×10^{-6} mbar, no oxidation of Pd was found in the whole range of temperatures investigated, up to 870 K, but catalytic oxidation of the carbon support film took place. The dependence of activity on particle size, in particular on the square of the mean particle diameter, suggests that the rate limiting step is connected with surface processes of dissociatively adsorbed oxygen on the metal surface.

Ni is oxidized to NiO at relatively low temperatures, e.g., at 600–700 K. However, above about 800 K, no oxidation was observed any longer. This is explained by increasing bulk diffusion of carbon, and segregation of graphite layers on the particle surfaces, which prevents oxidation of the Ni core. Apparently, segregated carbon is not oxidized on originally pure Ni, presumably because oxygen is not dissociatively adsorbed, in contrast to the case of Pd.

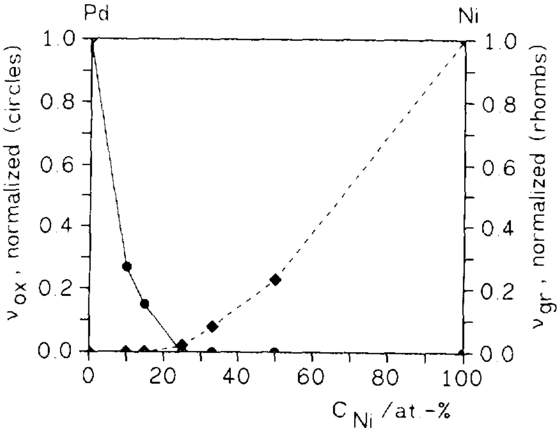

FIG. 12. Plot of the normalized activities for carbon oxidation ν_{ox}. (circles, left hand ordinate), and for graphitization ν_{gr}. (rhombs, right hand ordinate) vs the bulk concentration of Ni, C_{Ni}, in the particles. All data refer to a temperature of about 870 K and to an oxygen partial pressure of 5×10^{-6} mbar.

This view is supported by the results from Pd–Ni alloy particles with relatively low concentrations of Ni from 5 to about 10 at.%. The increasing tendency for precipitation of NiO with *decreasing* concentration of Ni can be explained by the increasing activation of adsorbed oxygen by dissociation due to the increasing abundance of Pd atoms at the particle surface. This would also be effective for some segregated carbon, which would be immediately gasified. With the concentration of Ni increasing above about 10 at.%, the tendency for dissociative adsorption of oxygen and, hence, the activity of gasification of the carbon support film decreases. Moreover, the diffusion of carbon atoms in the bulk and segregation at the surface of the particles increases. Thus, at a certain composition, oxidation of Ni is blocked and gasification of surface carbonis no longer effective, or is in quasi-equilibrium with segregation. At 870 K, this was the case for a concentration of about 25 at.% Ni. We did not find indications that this relative inactivity could be due to the existence of another stable alloy phase.

For even higher concentrations of Ni, carbon segregation dominates and leads to growth of graphite layers. As the diffusion of carbon atoms proceeds through the bulk of the particles, the graphite layers grow from the original surface of the particle towards its center. Concomitantly, the remaining metal core, rich in Ni, is driven out of the encapsulation and partly dispersed, similarly to the dispersion of the NiO, as was discussed above. Ni may be dissolved in the graphite layers on an atomic scale or evaporated, although no definite conclusions could be found so far.

Finally, the observed decrease of graphitization activity with increasing concentration of Pd indicates that diffusion of carbon atoms in the alloy is strongly hindered by Pd. In fact, we did not find any indication for an interaction of pure Pd with carbon under our experimental conditions.

REFERENCES

1. Heintz, E. A., and Parker, W. E., *Carbon* **4,** 473 (1966).
2. Fryer, J. R., *Nature (London)* **220,** 1121 (1968).
3. Anton, R., and Poppa, H., *in* "Proceedings, 10th International Congress on Electron Microscopy, Hamburg, 1982," p. 509. Deutsche Gesellschaft für Elektronenmikroskopie, Frankfurt, 1982.
4. Moorehead, R. D., Poppa, H., and Heinemann, K., *J. Vac. Sci. Technol.* **17**(1), 248 (1980).
5. Anton, R., Pennemann, B., and Schmidt, A., *in* "Proceedings, EUREM 88, Inst. Phys. Conf. Ser. No. 93," Vol. 2, p. 291. IOP Publishing Ltd. York, England, 1988.
6. Pennemann, B., and Anton, R., *J. Catal.* **118,** 417 (1989).
7. Su, H.-I., Heinemann, K., Poppa, H., and Boudart, M., *J. Solid State Chem.* **106,** 55 (1993).
8. Avalos-Borja, M., Su, D., Ponce, F. A., Tramontana, J. C., Guo, Q.-H., Heinemann, K., Poppa, H., and Boudart, M., *Mater. Res. Soc. Symp. Proc.* **139,** 81 (1989).
9. Anton, R., Eggers, H., and Veletas, J., *Thin Solid Films* **226,** 39 (1993).
10. Baker, R. T. K., and Sherwood, R. D., *in* "Proceedings, 39th Annual EMSA Meeting, 1981," (G. W. Bailey, Ed.), p. 76. Claitor's Publishing Division, Baton Rouge, LA, 1981.
11. Marsh, H., and Warburton, A. P., *J. Appl. Chem.* **20,** 113 (1970).
12. Holstein, W. L., Moorhead, R. D., Poppa, H., and Boudart, M., *in* "Chemistry and Physics of Carbon," (P. L. Walker, Ed.), Vol. 18, p. 139. Dekker, New York, 1982.
13. Lamber, R., Jaeger, N., and Schultz-Ekloff, G., *Surf. Sci.* **197,** 402 (1988).
14. Benndorf, C., Klatte, G., and Thieme, F., *Surf. Sci.* **152–153,** 399 (1985).
15. Wandelt, K. and Ertl, G., *Z. Naturforsch* **31,** 205 (1976).
16. Anton, R., and Schweinfest, R., in preparation.
17. Anton, R., *in* "Proceedings, XIth International Congress on Electron Microscopy, Kyoto 1986," *J. Electron Microsc.* **35,** Supplement, Vol. 1, p. 339 (1986).
18. Anton, R., Reetz, O., and Schmidt, A. A., *Ultramicroscopy* **41,** 303 (1992).
19. Anton, R., Schmidt, A., and Schünemann, V., *Vacuum* **41,** 1101 (1990).
20. Schmidt, A., Schünemann, V., and Anton, R., *Phys. Rev. B* **41,** 11875 (1990).
21. Schmidt, A., Spode, M., Heinrich, J., and Anton, R., *Thin Solid Films* **196,** 253 (1991).
22. Tyson, W. R., and Miller, W. A., *Surf. Sci.* **62,** 267 (1977).
23. Weast, R. C., and Linde, D. R. (Eds.), "Handbook of Chemistry and Physics," CRC Press, Boca Raton, FL, 1989.
24. Yang, R. T., Goethel, P. J., Schwartz, J. M., and Lund, C. R. F., *J. Catal.* **122,** 206 (1990).
25. Bartholomew, C. H., *in* "Catalysis" (Specialist Periodical Report, The Royal Society of Chemistry), Vol. 10, p. 41, 1993.
26. Pietersen, C. A., Mesters, C. M. A. M., Habraken, F. H. P. M., Gijzeman, O. L. J., Geus, J. W., and Bootsma, G. A., *Surf. Sci.* **107,** 353 (1981).